TABLE 4.1: Key characteristics of water vapour treatment in reanalyses

Reanalysis	Assimilation of satellite humidity radiances?	Highest level of analyzed WV	Stratospheric WV used in radiative transfer	Stratospheric WV treatment	Stratospheric methane oxidation parameterization
NCEP R1	No	300 hPa	Climatology	None	N/A
NCEP R2	No	300 hPa	Climatology	None	N/A
CFSR	Yes	250 hPa	Analyzed. Negative values set to 0.1 ppmv	Prognostic	None
ERA-40	Yes	Diagnosed tropopause. Radiosonde humidity generally used to 300 hPa	Analyzed	Prognostic	Relaxation to 6 ppmv WV
ERA-I	Same as ERA-40	Same as ERA-40	Same as ERA-40	Same as ERA-40	Relaxation to 6.8 ppmv WV
JRA-25	Yes	100 hPa	Constant 2.5 ppmv used	None. WV set to 2.5 ppmv.	None
JRA-55	Same as JRA-25	Same as JRA-25	Same as JRA-25	Same as JRA-25	Same as JRA-25
MERRA	Yes	300 hPa	Analyzed	3-day relaxation to zonal-mean monthly-mean satellite-based climatology	None
MERRA-2	Same as MERRA	Same as MERRA	Same as MERRA	Same as MERRA	Same as MERRA

TABLE 4.2: Key characteristics of ozone treatment in reanalyses

Reanalysis	Primary TCO data source	Vertical profile data	Stratospheric O_3 used in radiative transfer	Stratospheric O_3 treatment	Photochemical parameterization
NCEP R1	None	None	Climatology	None	N/A
NCEP R2	None	None	Climatology	None	N/A
CFSR	SBUV	SBUV	Analyzed	Prognostic	CHEM2D-OPP
ERA-40	TOMS	SBUV	Climatology	Prognostic	CD86
ERA-I	Same as ERA-40	SBUV, GOME, MLS, MIPAS	Same as ERA-40	Same as ERA-40	Same as ERA-40
JRA-25	TOMS (1979 - 2004)[1] OMI (2004 -)	Nudging to climatology profile	Daily values provided by offline CCM	Daily values provided by offline CCM	N/A
JRA-55	Same as JRA-25	None	Same as JRA-25	Same as JRA-25	Same as JRA-25
MERRA	SBUV	SBUV	Analyzed	Prognostic	Stajner et al. (2008)
MERRA-2	SBUV (1980 – 9/2004) OMI (9/2004 –)	SBUV, MLS	Same as MERRA	Same as MERRA	Same as MERRA

[1] Offline CCM nudged to TOMS/OMI data.

TABLE 4.3: Ozone hole mean area model differences from TOMS/OMI for 21 September to 20 October, 1981–2010

Reanalysis	Mean Difference[1] (million km^2)	(%)	Root-mean-square difference[1] (million km^2)	(%)
MERRA	-2.6	-14.2	5.0	79.3
MERRA-2	-0.6	-3.0	2.8	44.5
ERA-Interim	-0.8	-4.3	0.9	14.6
ERA-40[2]	-3.8	-21.8	5.1	75.4
JRA-55	-1.0	-5.2	0.6	10.2
NCEP-CFSR	-0.7	-3.7	0.9	14.1

[1]TOMS_OMI average = 19.6 million km^2, standard deviation = 6.9 million km^2)

[2]ERA-40 statistics here encompasses the period from 1981 through 2001.

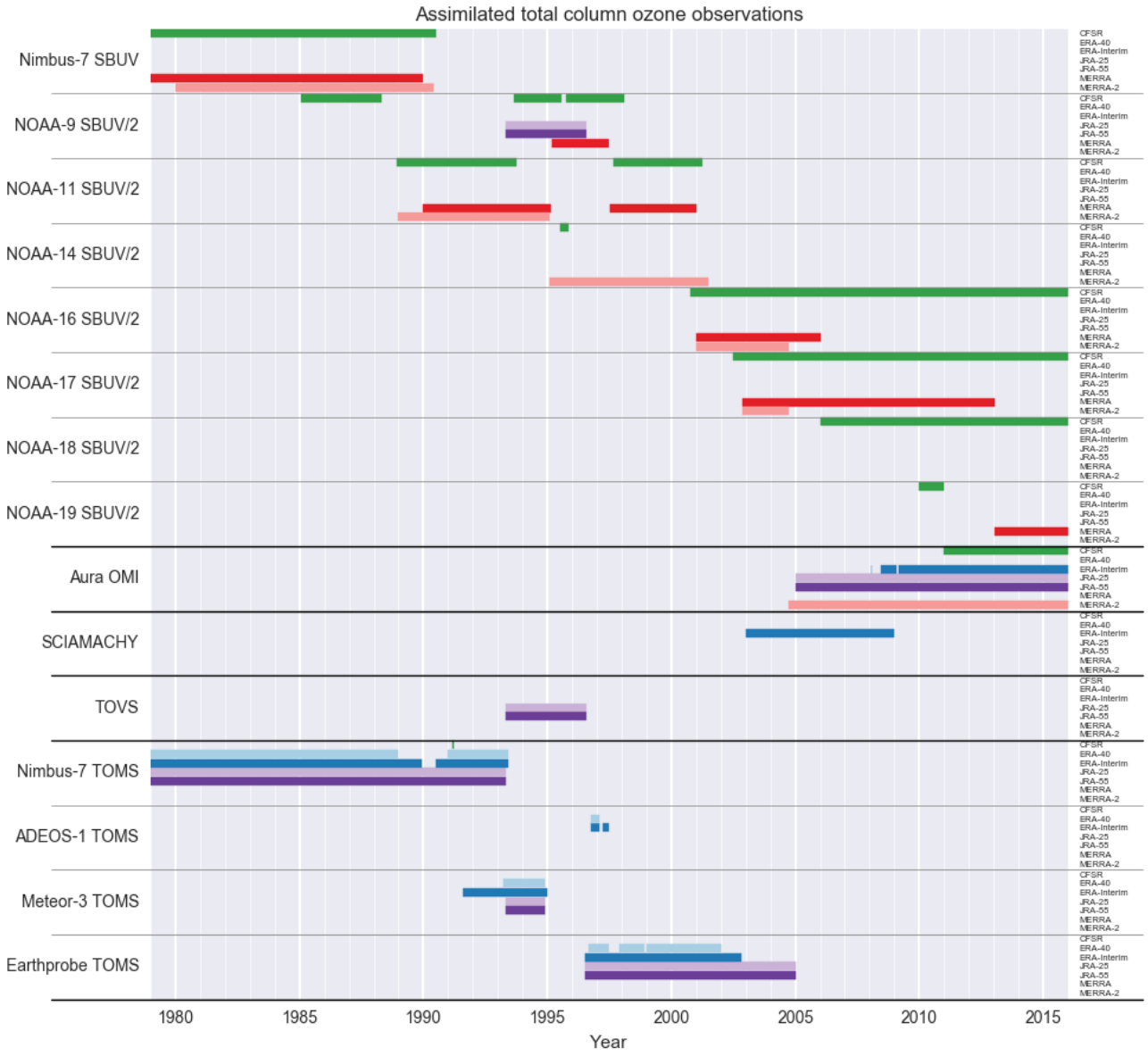

Figure 4.1. Total column ozone data assimilated by reanalyses.

Figure 4.2. Ozone vertical profile observations assimilated by reanalyses.

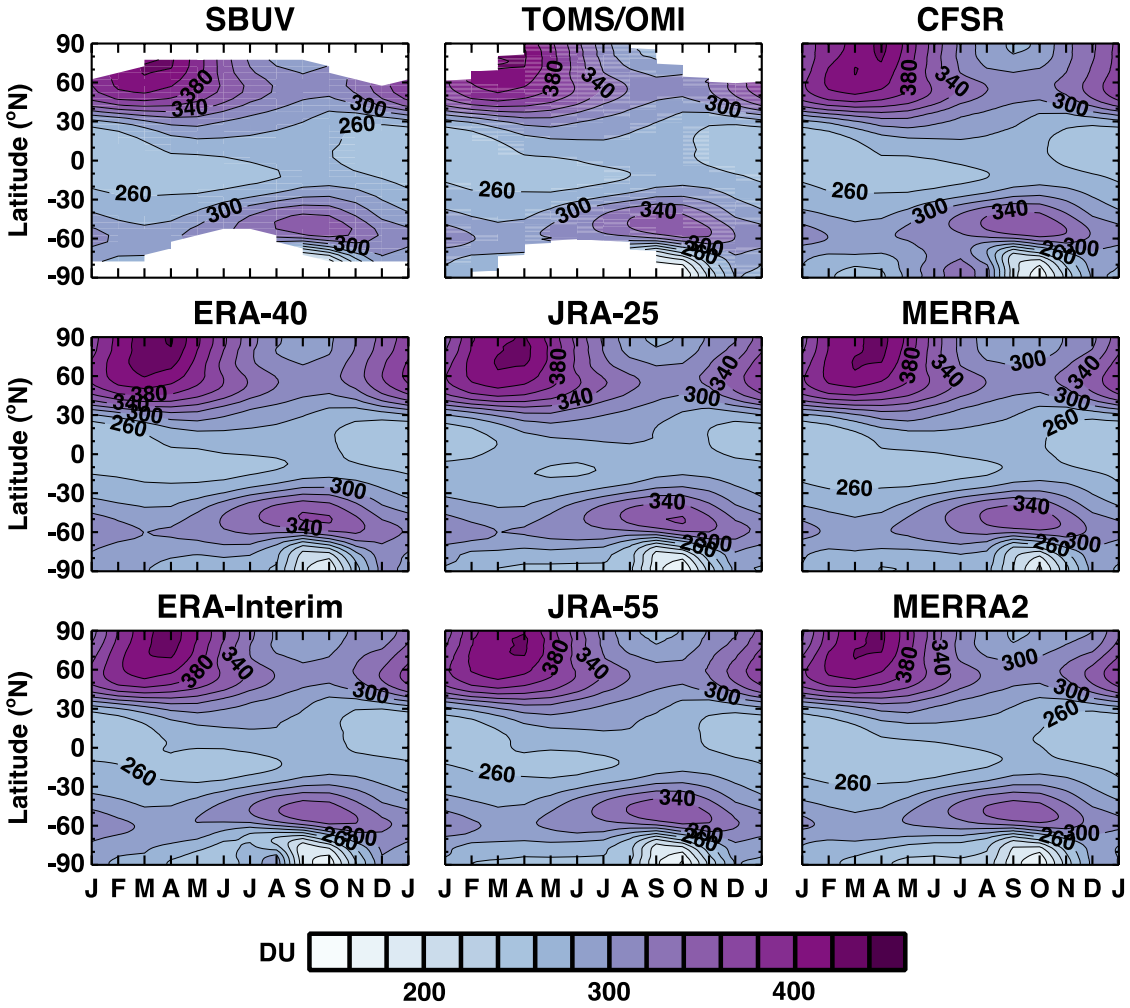

Figure 4.3. Zonal- and monthly-mean total column ozone climatology over 1981–2010 for observations and reanalyses (with the exception of ERA-40 that is only available until Aug 2002).

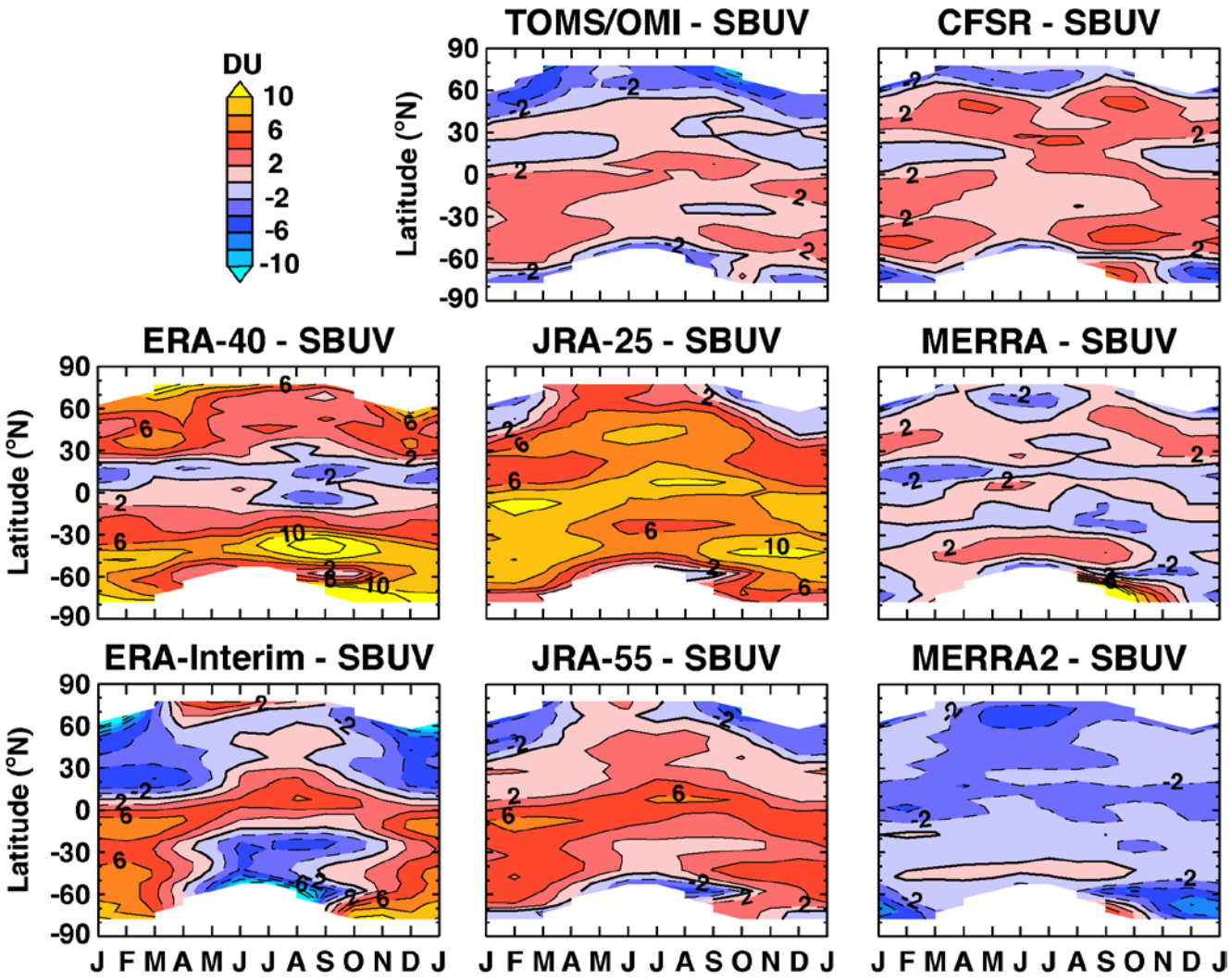

Figure 4.4. Zonal- and monthly-mean total column ozone climatology (1981–2010) differences between reanalyses and SBUV. Also included is the TOMS/OMI difference with SBUV.

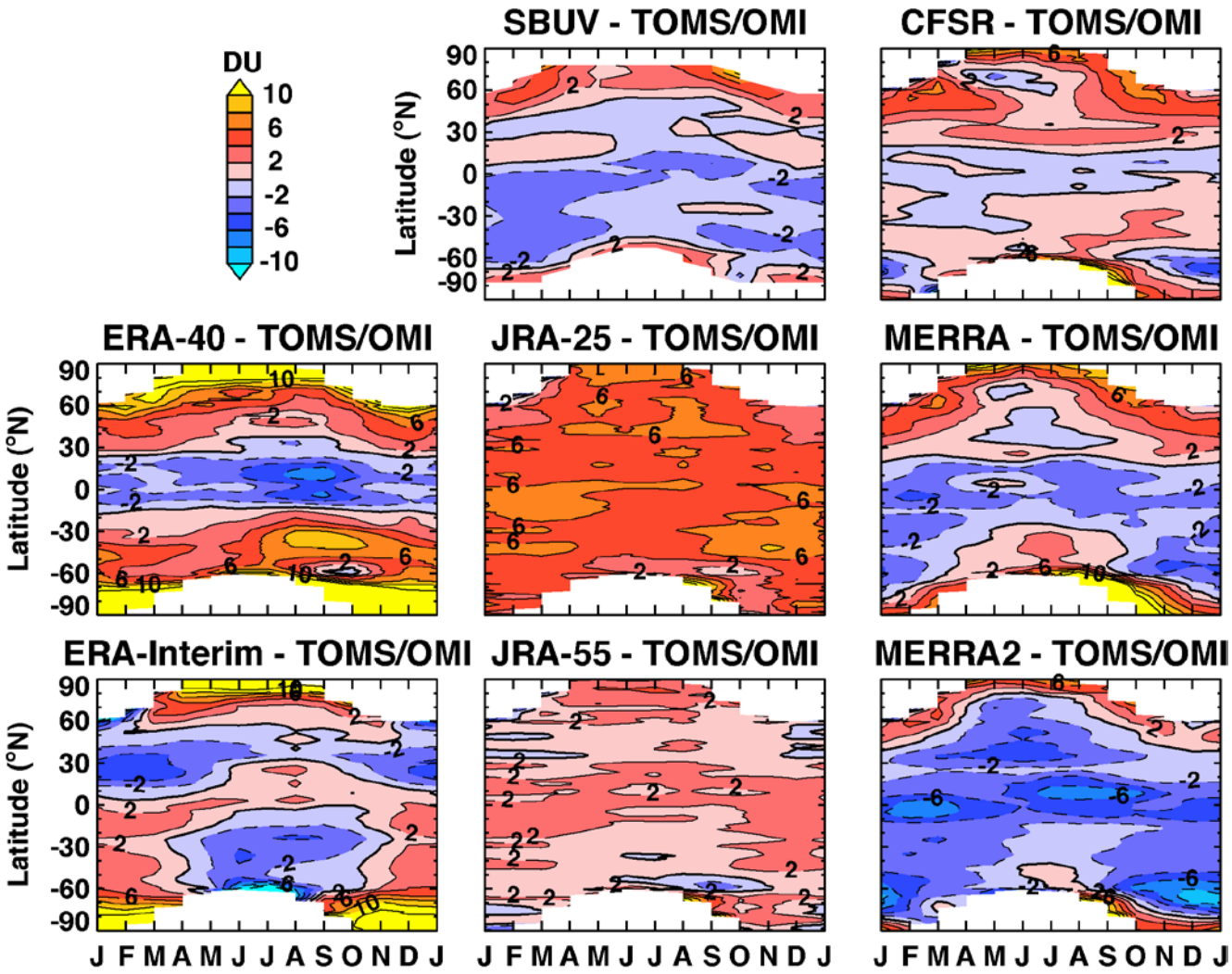

Figure 4.5. Same as Fig. 4.4, but for TOMS/OMI.

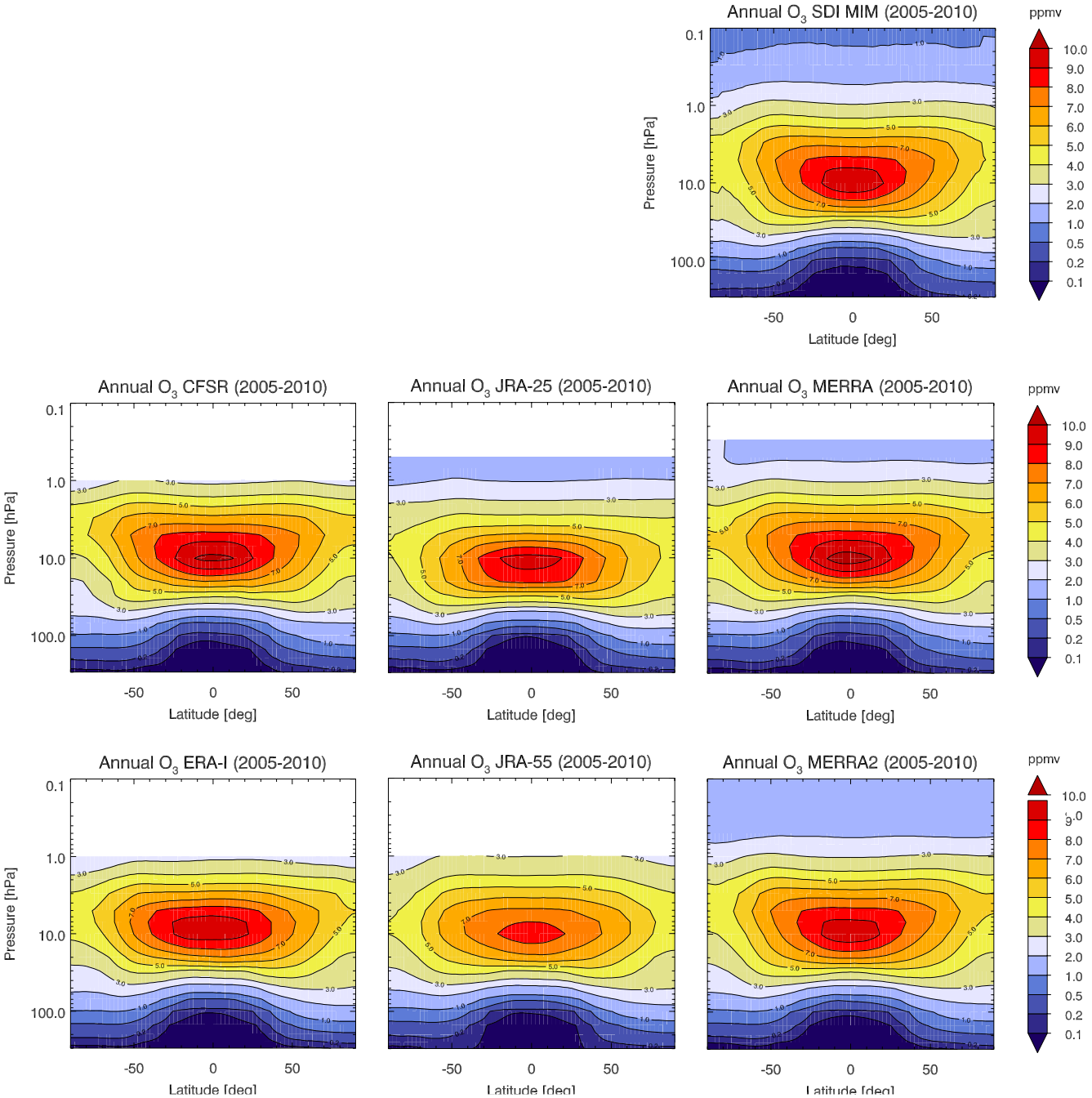

Figure 4.6. Multi-annual mean zonal mean cross sections of ozone averaged over 2005-2010 for the SPARC Data Initiative multi-instrument mean (MIM) (upper right) and the different reanalyses.

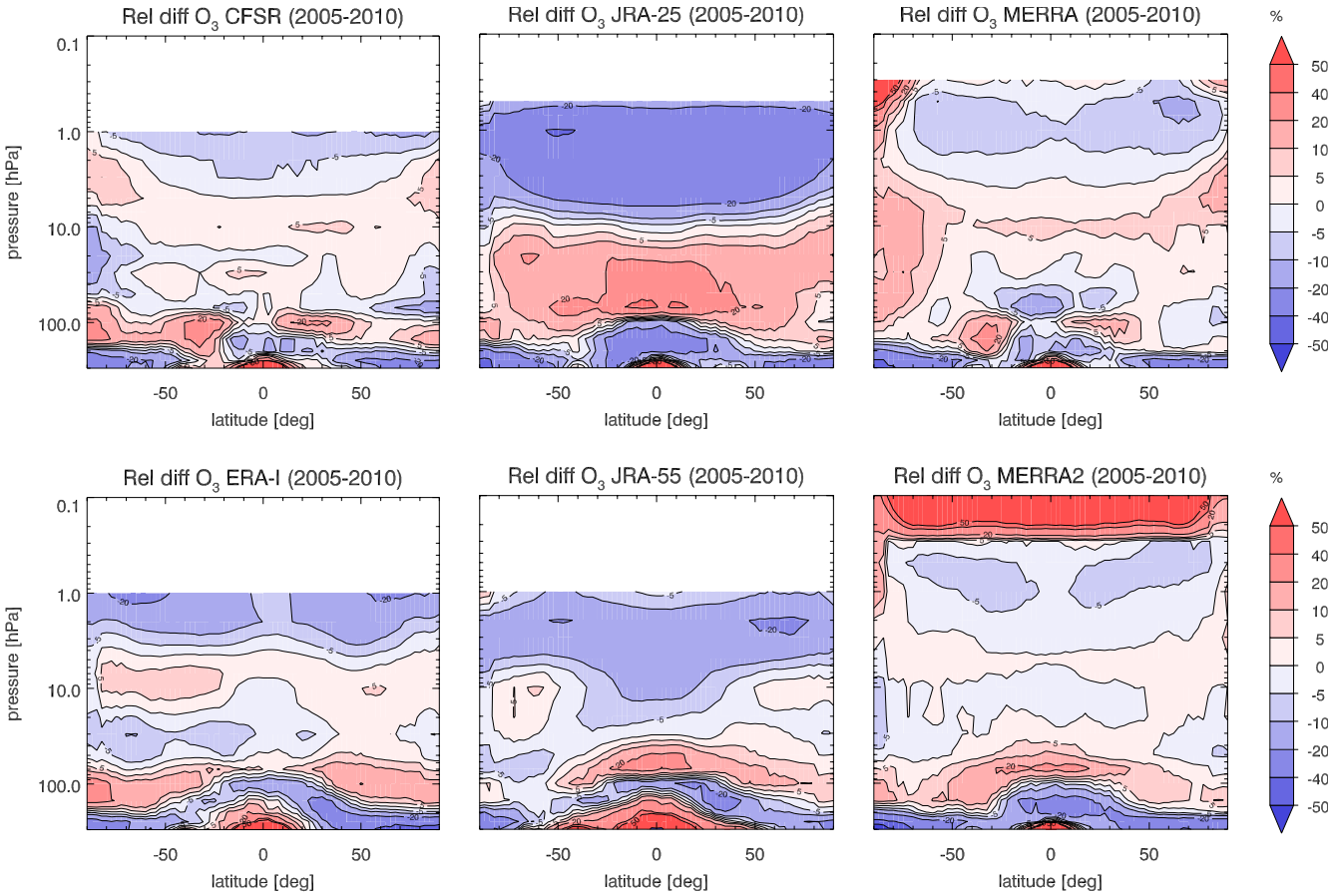

Figure 4.7. Relative percentage differences of the multi-annual mean zonal mean cross sections of ozone averaged over 2005-2010 between the SPARC Data Initiative multi-instrument mean (MIM) and the different reanalyses using (R_i-MIM)/MIM*100.

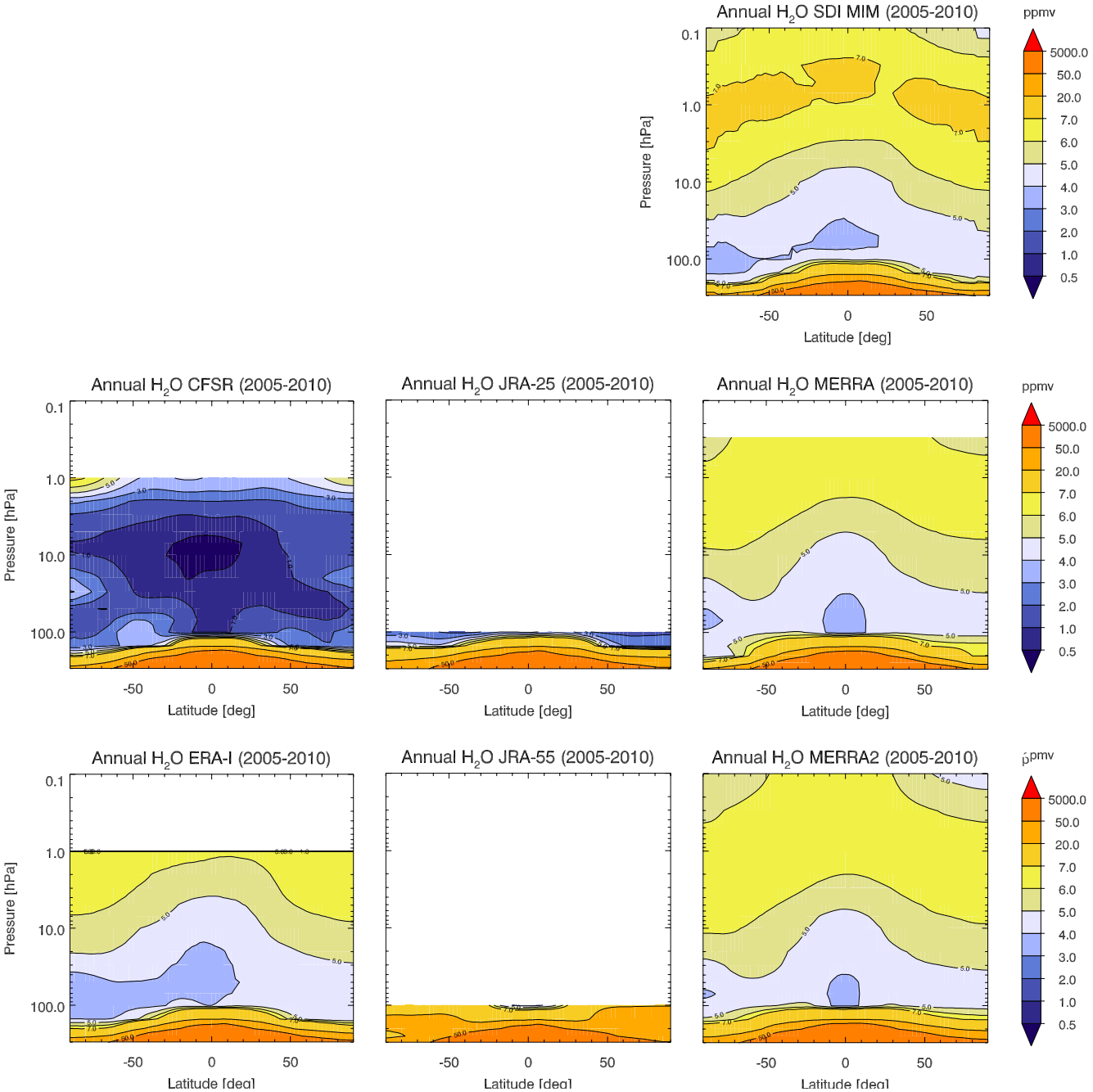

Figure 4.8. Multi-annual mean zonal mean cross sections of water vapour averaged over 2005-2010 for the SPARC Data Initiative multi-instrument mean (MIM) (upper right) and the different reanalysis.

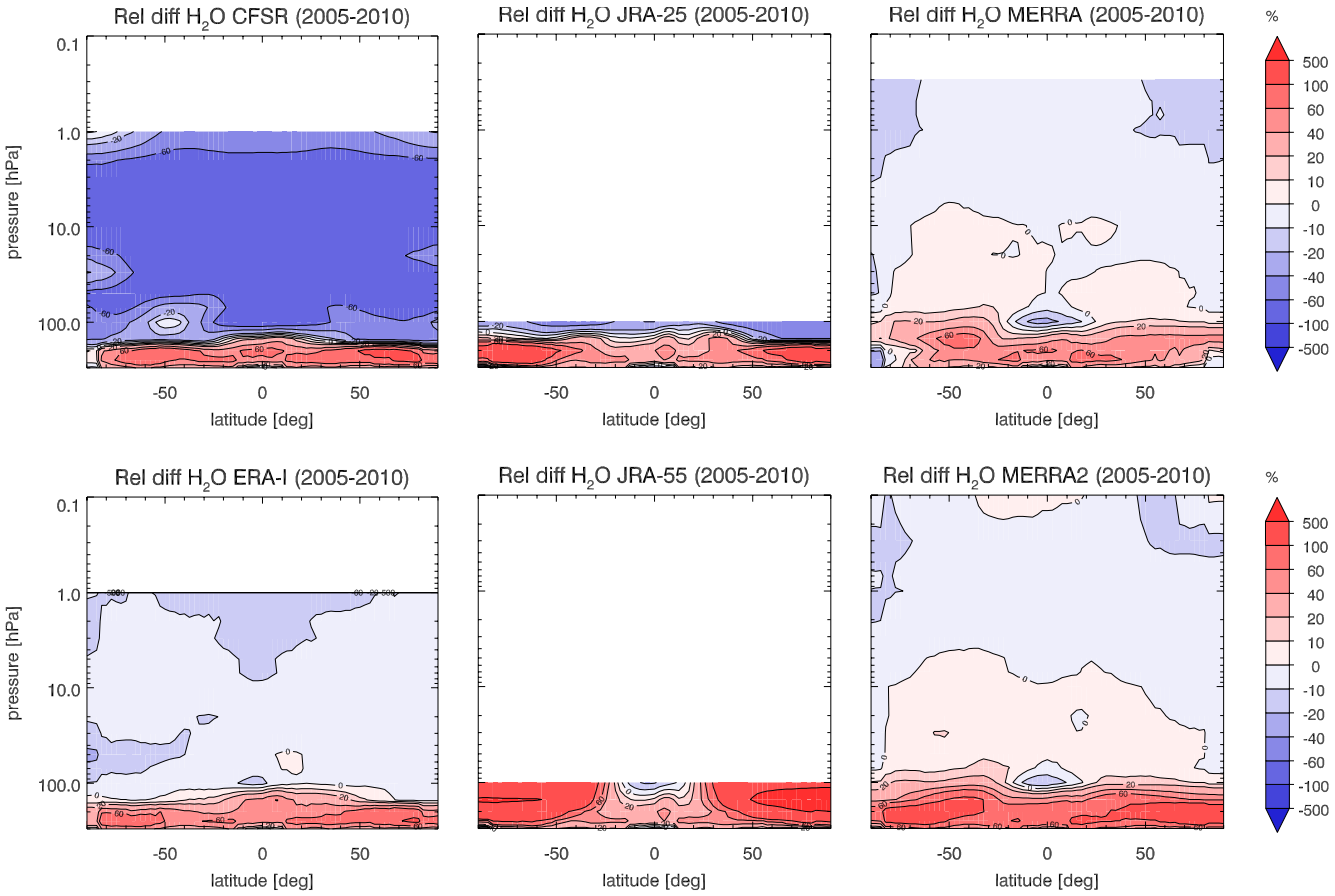

Figure 4.9. Relative percentage differences of the multi-annual mean zonal mean cross sections of water vapour averaged over 2005-2010 between the SPARC Data Initiative multi-instrument mean (MIM) and the different reanalyses using (R_i-MIM)/MIM*100.

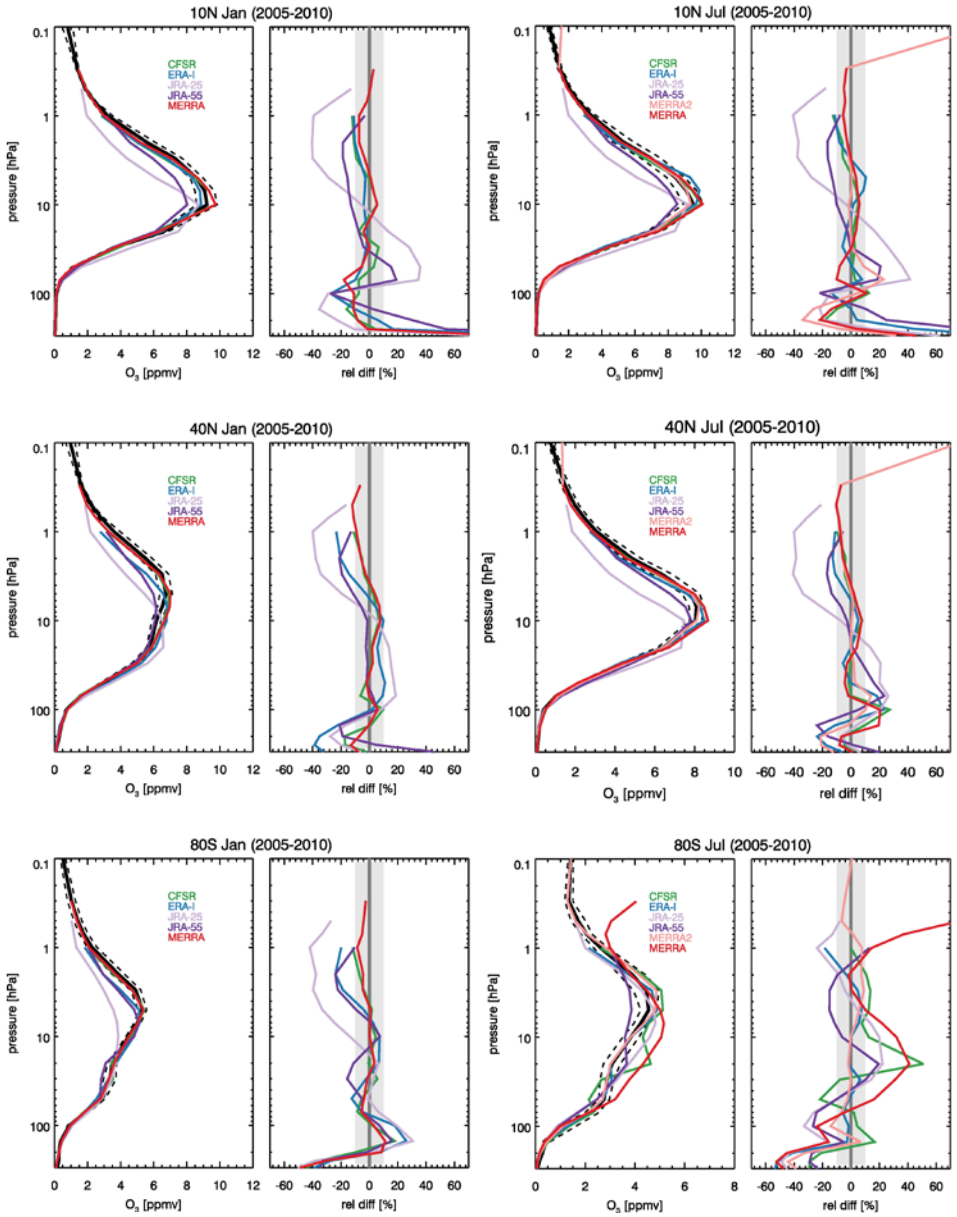

Figure 4.10. Monthly mean vertical profiles of ozone for January (left column) and July (right column) at different latitudes averaged over 2005-2010, for the SDI MIM (black) and the different reanalysis (coloured). Absolute values are shown in the left hand panels, relative differences between each reanalysis and the MIM in the right hand panels using (R_i-MIM)/MIM*100.

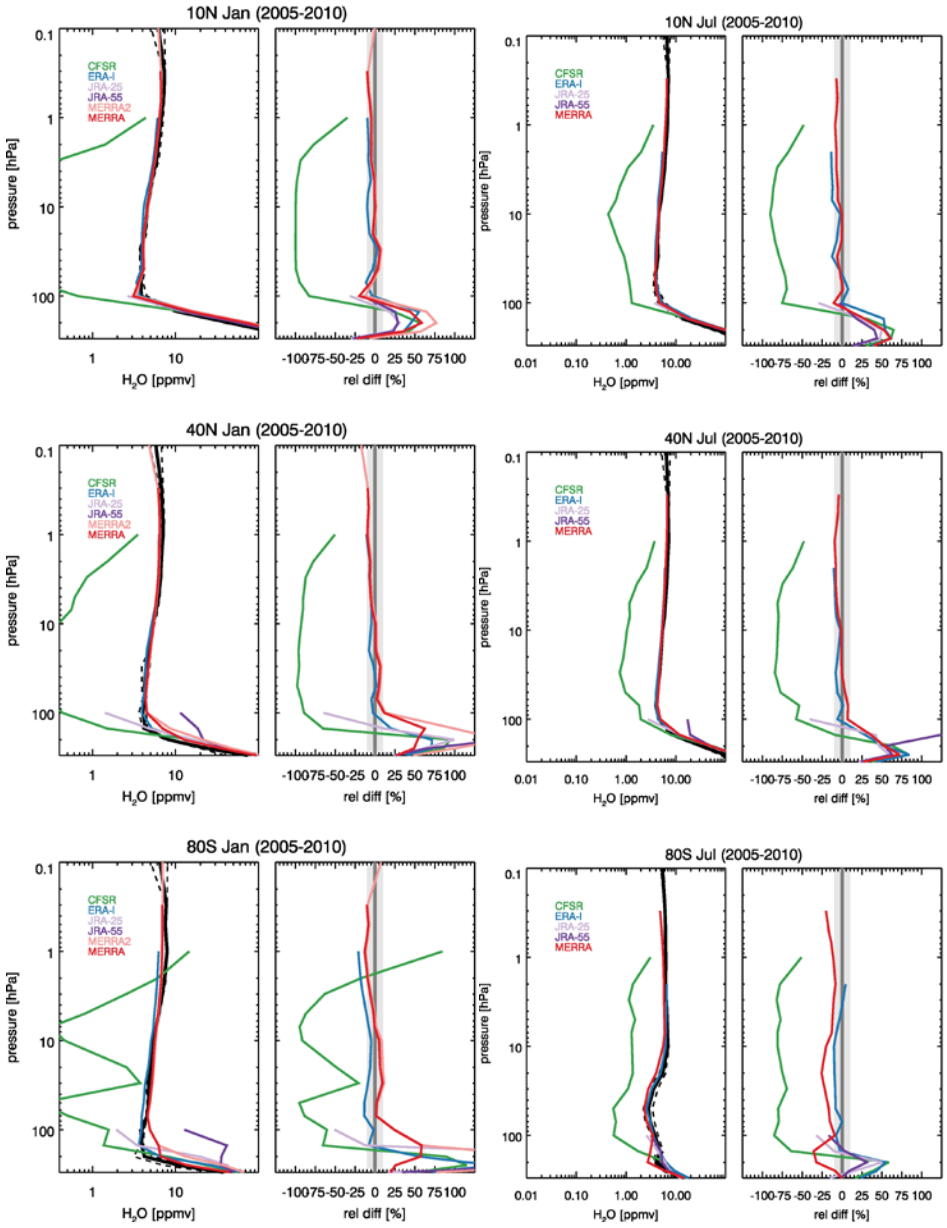

Figure 4.11. Monthly mean vertical profiles of water vapour for January (left column) and July (right column) at different latitudes averaged over 2005-2010, for the SDI MIM (black) and the different reanalysis (coloured). Absolute values are shown in the left hand panels, differences between each reanalysis and the MIM in the right hand panels using (R_i-MIM)/MIM*100.

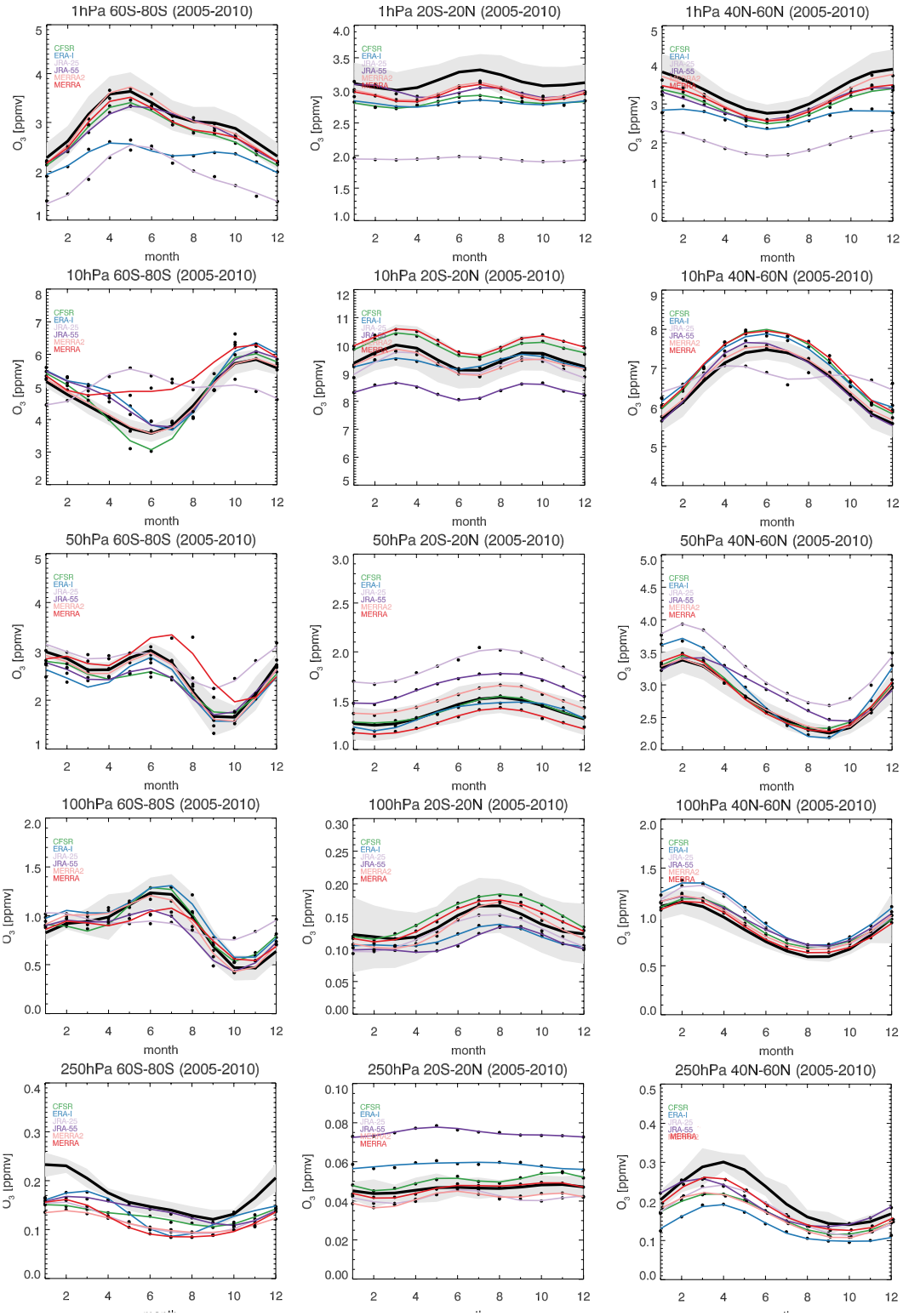

Figure 4.12. Seasonal cycle of ozone averaged over 2005-2010 for the SPARC Data Initiative multi-instrument mean (MIM, black) and the different reanalysis (coloured) at different pressure levels (top to bottom: 1, 10, 50, 100, and 250 hPa) and latitude ranges (left to right: 60S-80S, 20S-20N, 40N-60N). Grey shading indicates the observational uncertainty (±1-sigma). The dots are the monthly mean values, and the lines are fits including annual and semi-annual components to the available data points.

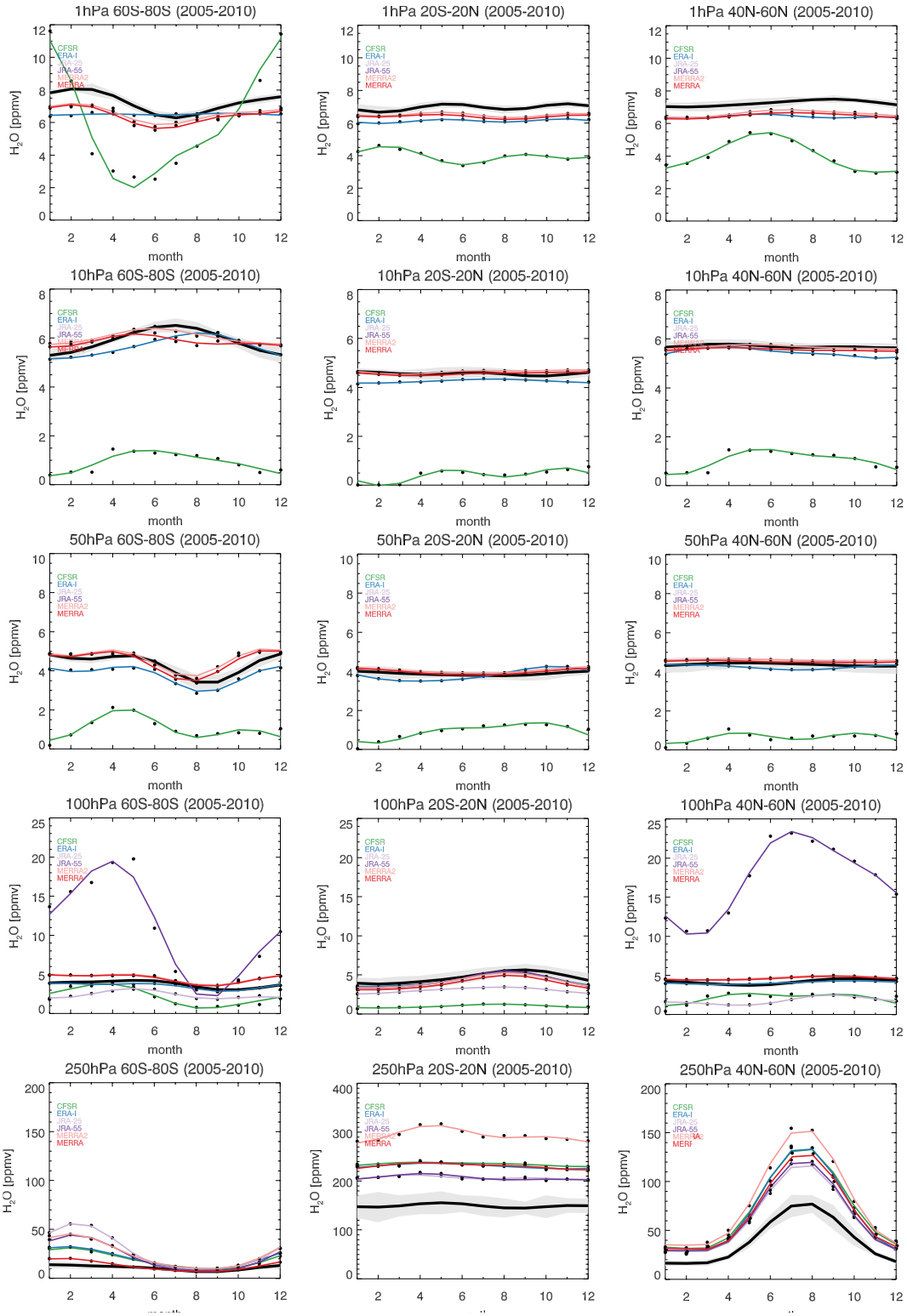

Figure 4.13. Seasonal cycle of water vapour averaged over 2005-2010 for the SPARC Data Initiative multi-instrument mean (MIM, black) and the different reanalysis (coloured) at different pressure levels (top to bottom: 1, 10, 50, 100, and 250 hPa) and latitude ranges (left to right: 60S-80S, 20S-20N, 40N-60N). Grey shading indicates the observational uncertainty (±1-sigma). The dots are the monthly mean values, and the lines are fits including annual and semi-annual components to the available data points.

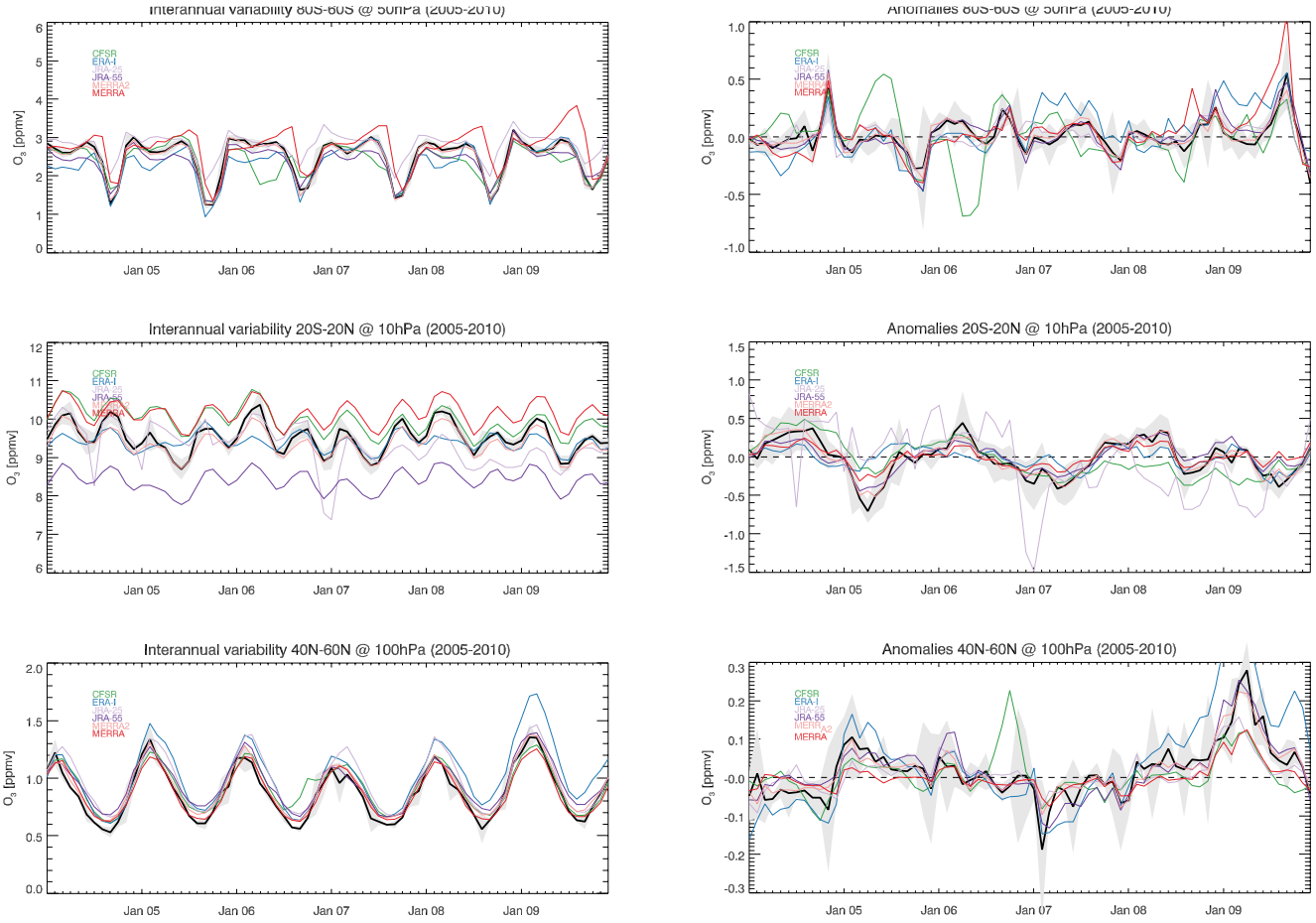

Figure 4.14 Interannual variability (left column) and deseasonalized anomalies (right column) for ozone between 2005 and 2010 for the SPARC Data Initiative multi-instrument mean (MIM, black) and the different reanalysis (coloured). Results are shown for different pressure levels and latitude ranges (top to bottom: 50 hPa at 60S-80S, 10 hPa at 20S-20N, and 100 hPa at 40N-60N). Grey shading indicates the observational uncertainty (±1-sigma).

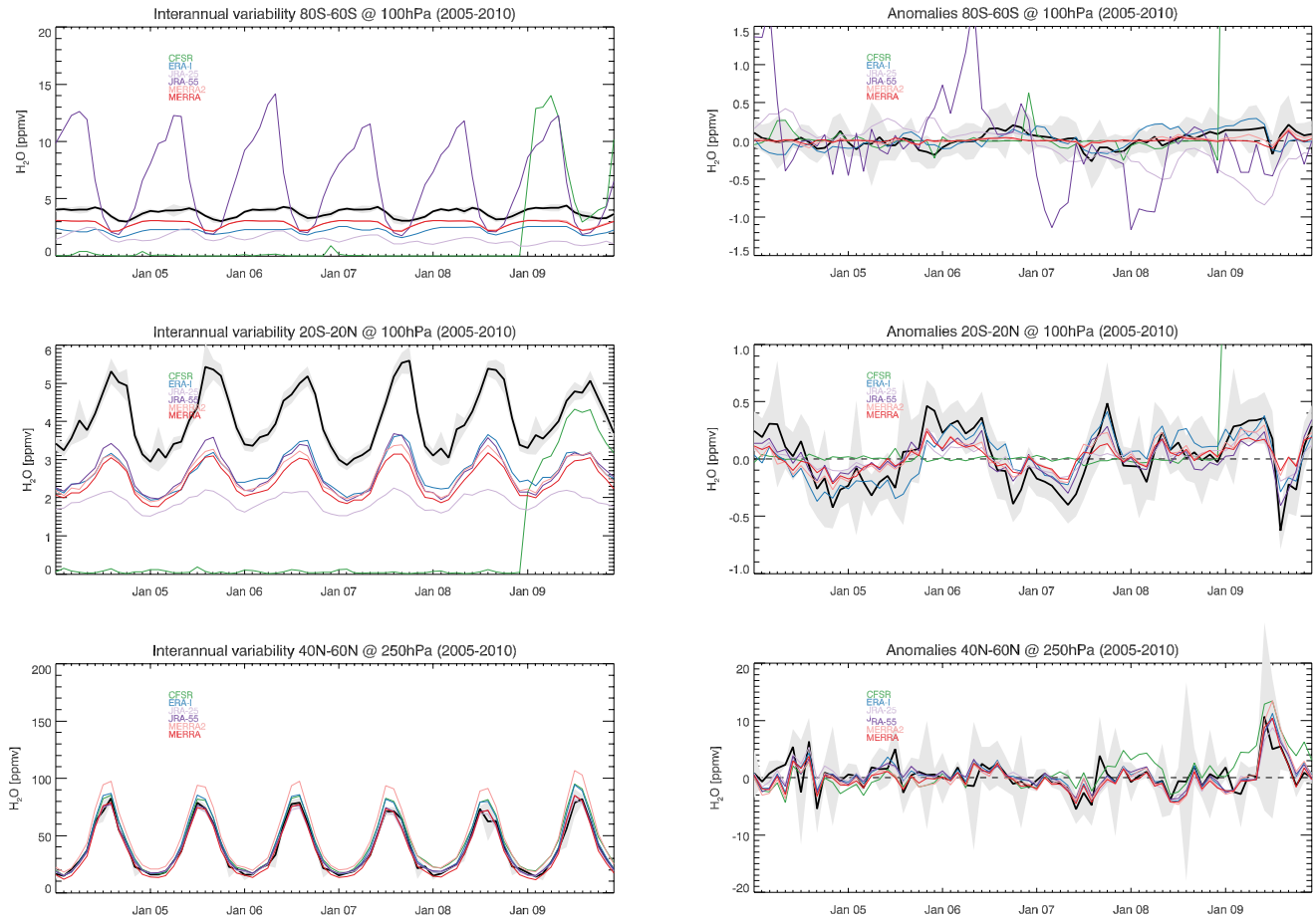

Figure 4.15. Interannual variability (left column) and deseasonalized anomalies (right column) for water vapour between 2005 and 2010 for the SPARC Data Initiative multi-instrument mean (MIM, black) and the different reanalysis (coloured). Results are shown for different pressure levels and latitude ranges (top to bottom: 100 hPa at 60S-80S, 100 hPa at 20S-20N, and 250 hPa at 40N-60N). Grey shading indicates the observational uncertainty (±1-sigma).

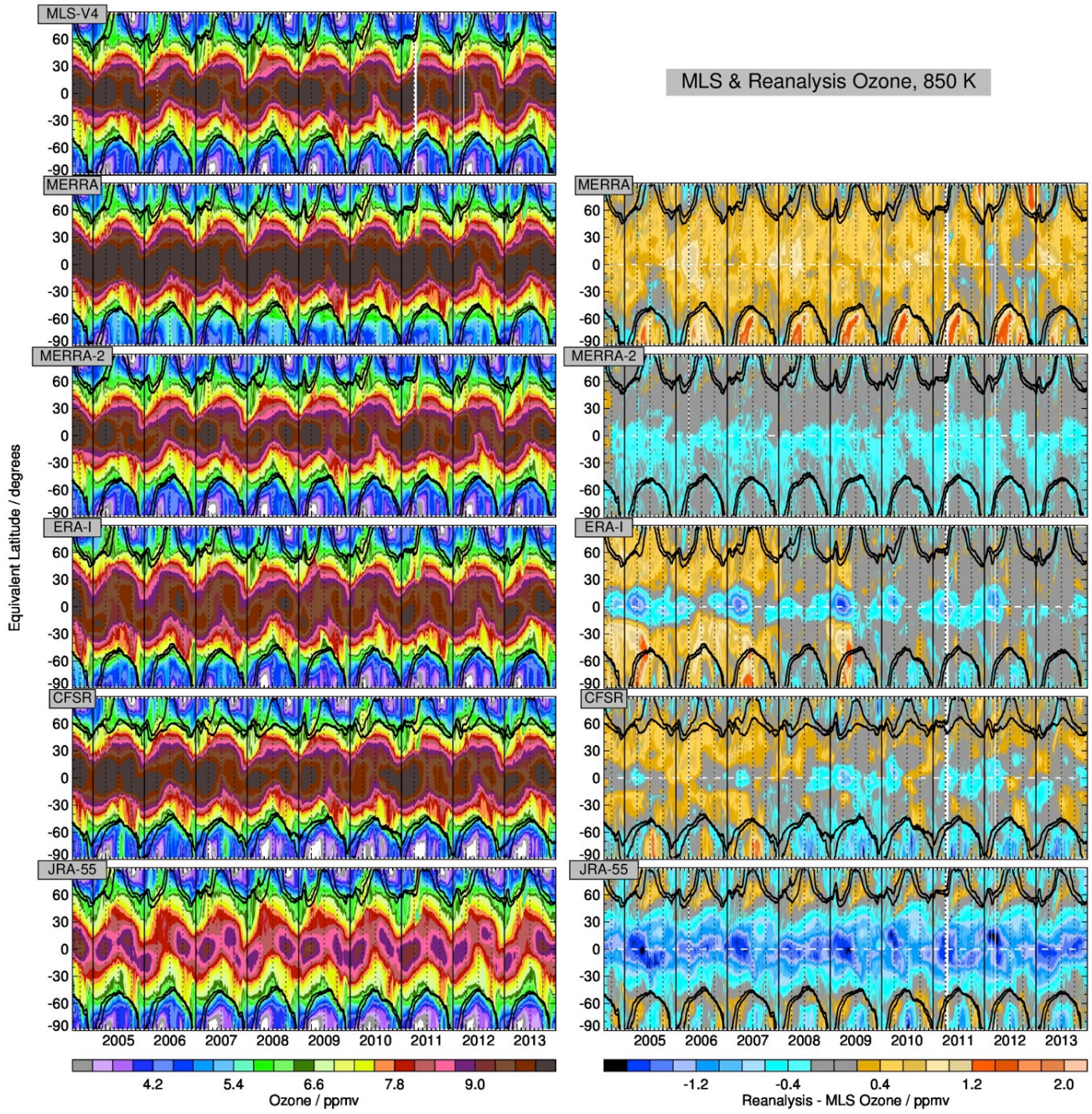

Figure 4.16. Comparison of equivalent latitude-time evolution of reanalysis ozone with that from MLS on the 850K isentropic surface (near 30km, 10hPa) during the Aura mission (September 2004 through December 2013). (Left) Mixing ratios (ppmv) for (top to bottom) MLS and the MERRA, MERRA-2, ERA-Interim, CFSR, and JRA-55 reanalyses. (Right) differences (ppmv) between each reanalysis and MLS (expressed as Reanalysis minus MLS). Overlays are scaled PV (Manney et al., 1994) contours of 1.4 and 1.6 x 10^{-4} s^{-1}, indicating the polar vortex edge region in winter, from the corresponding reanalysis, with MERRA contours overlaid on the MLS panel.

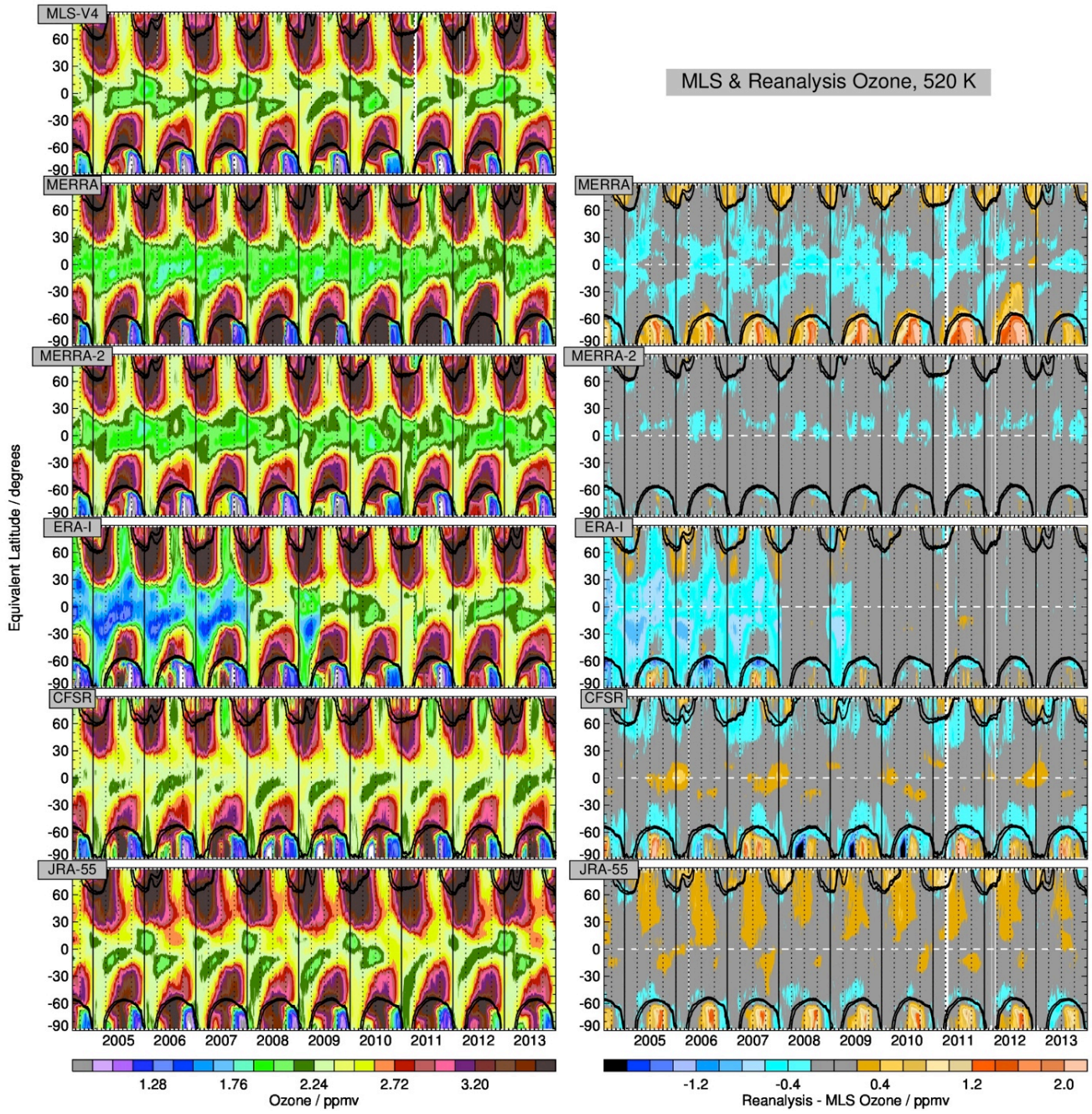

Figure 4.17. As is Figure 4.15, but for 520K (near 20km, 50hPa).

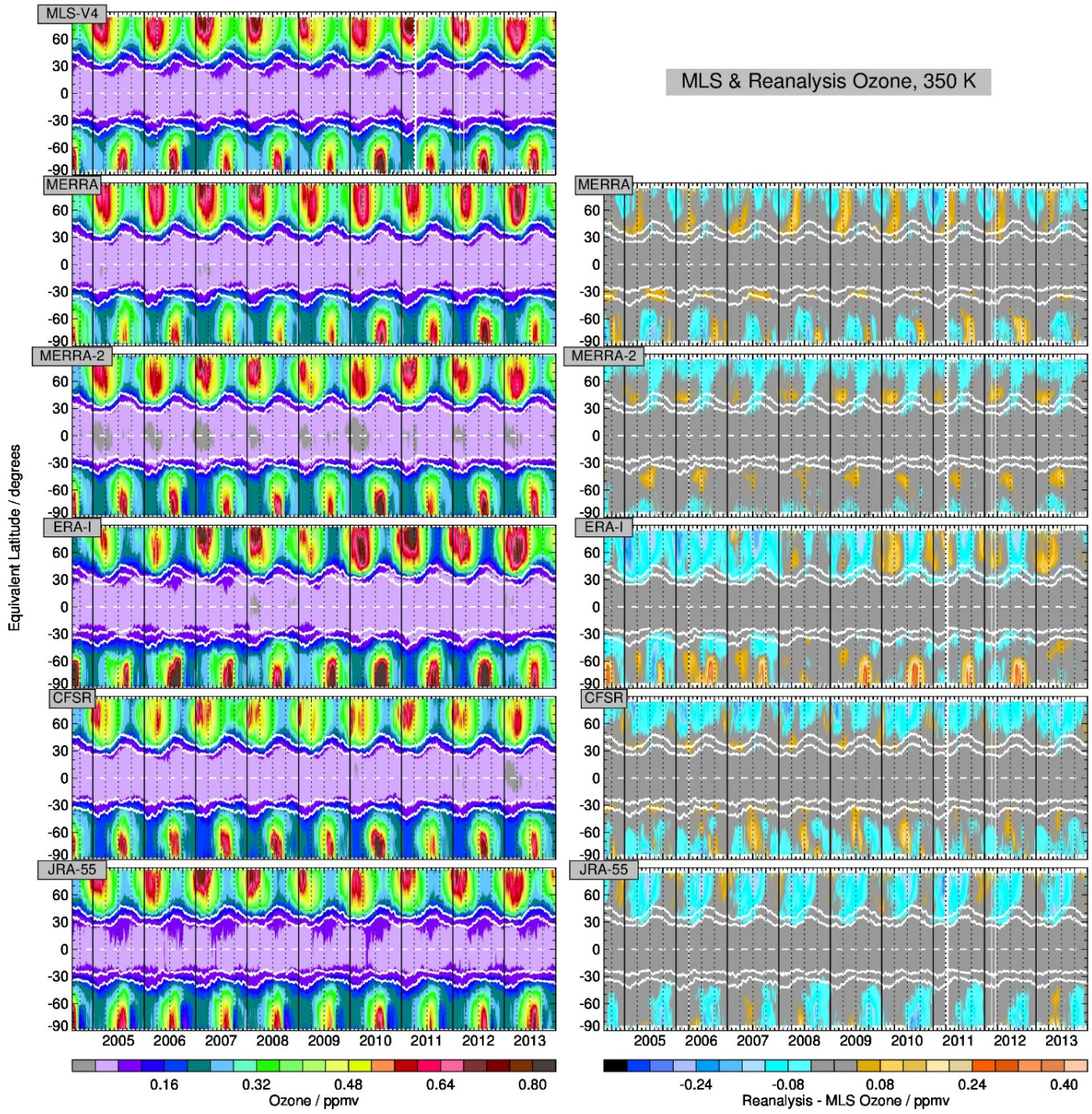

Figure 4.18. As is Figure 4-15, but for 350K (near 11km, 200hPa), and without vortex-edge sPV contours. The white contours are PV values of magnitude 1.5 and 4.5PVU, bounding the range commonly used to define the dynamical tropopause.

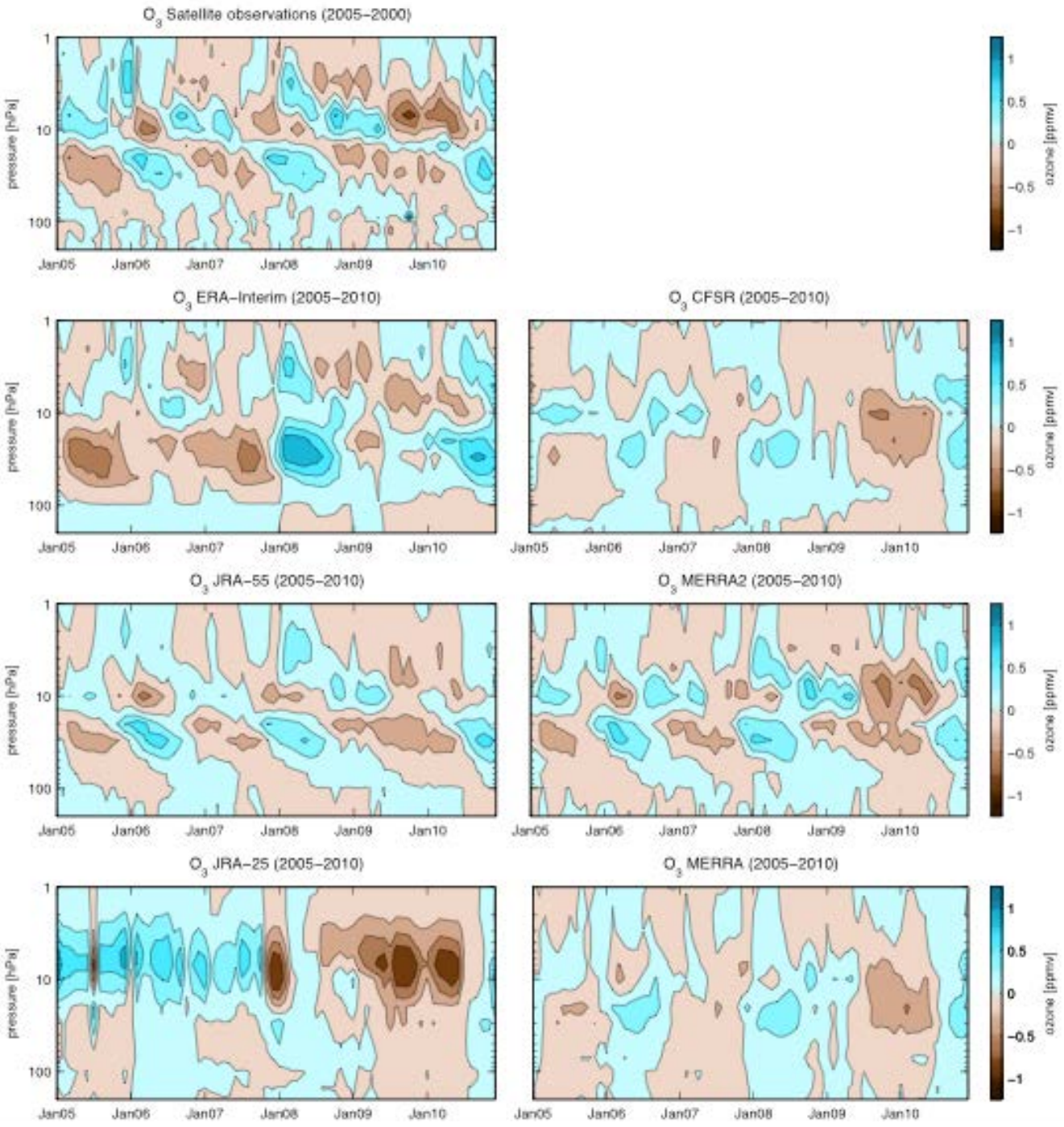

Figure 4.19. QBO signal for 2005-2010. Altitude-time sections of deseasonalized ozone anomalies for 10°S-10°N from 2005 to 2010 are shown. The observations are based on three satellite data sets.

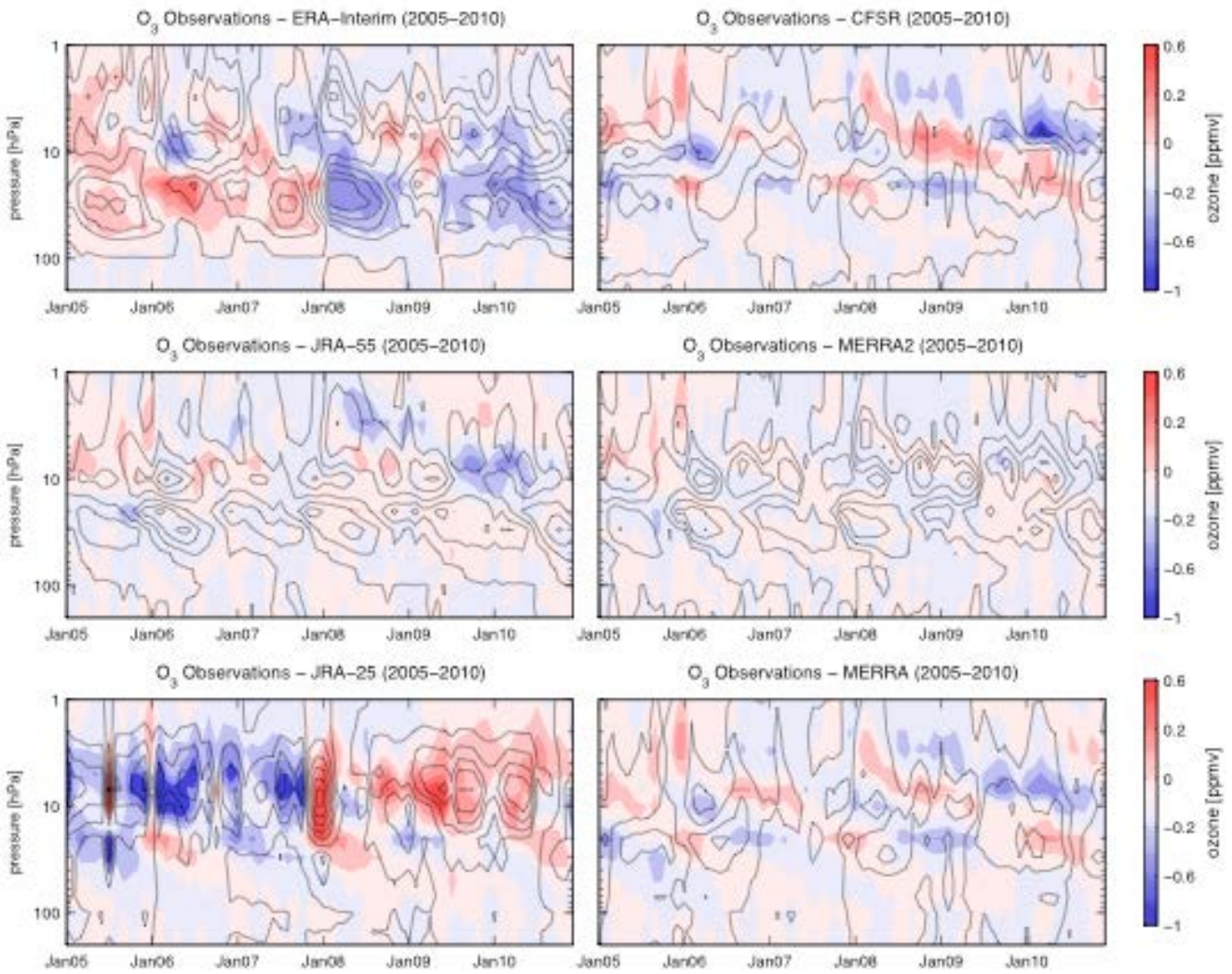

Figure 4.20. Differences with respect to observations for QBO ozone signal for 2005-2010. Altitude-time section of ozone anomaly differences between the observational data set and each reanalysis are shown by color contours. The black contours present the ozone anomalies of the respective reanalysis data set.

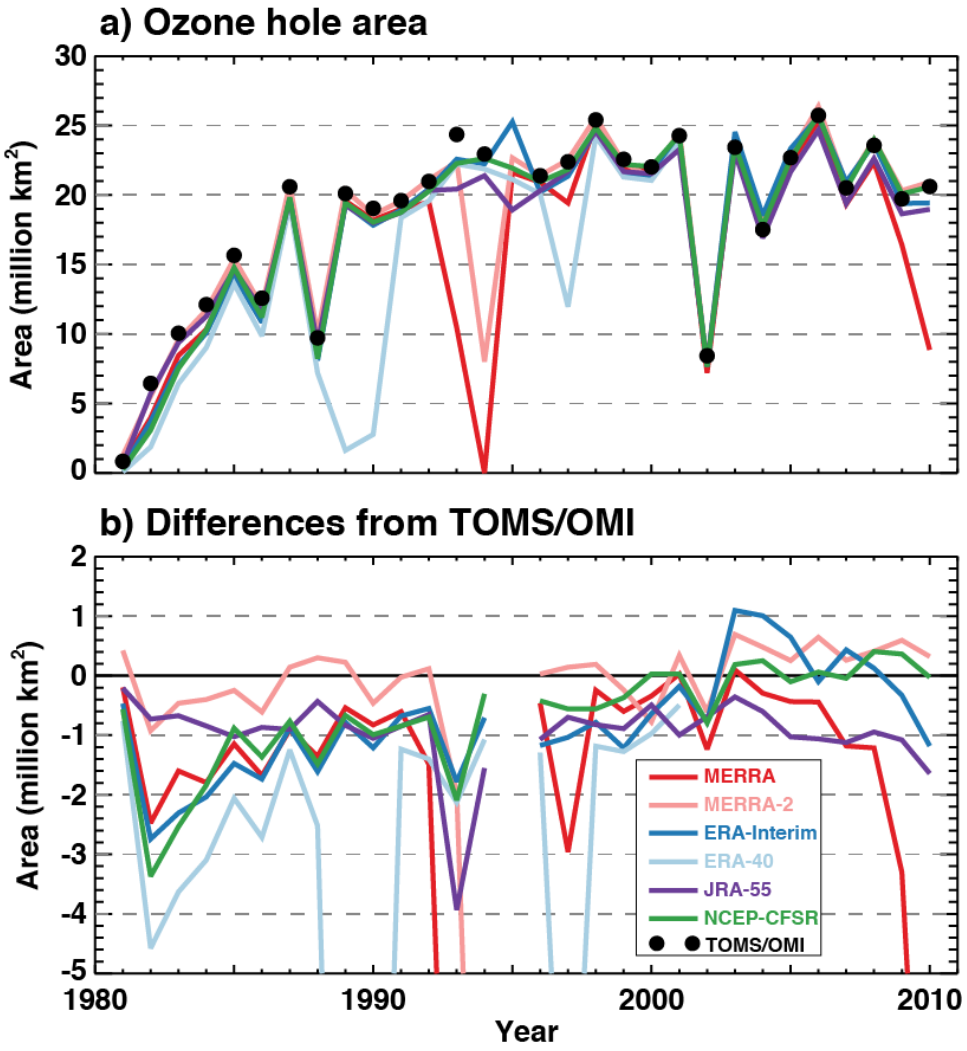

Figure 4.21. (a) Ozone hole mean area calculated from six models and from TOMS/OMI observations for 21 September – 20 October 1981–2010. (b) Differences between the reanalyses and TOMS/OMI TCO observations.

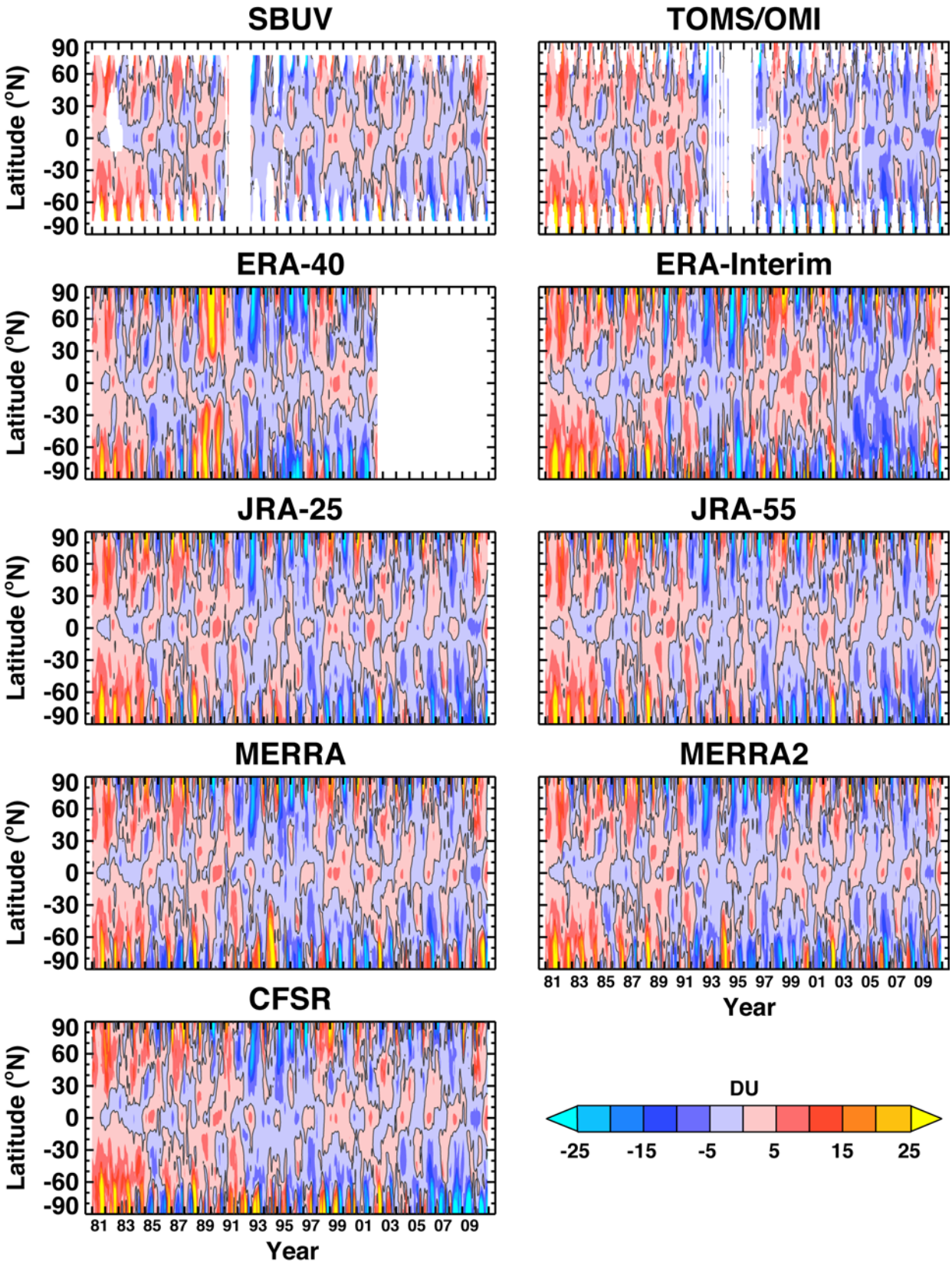

Figure 4.22. Departures of zonal- and monthly-mean total column ozone from climatology (1981–2010) for observations and reanalyses.

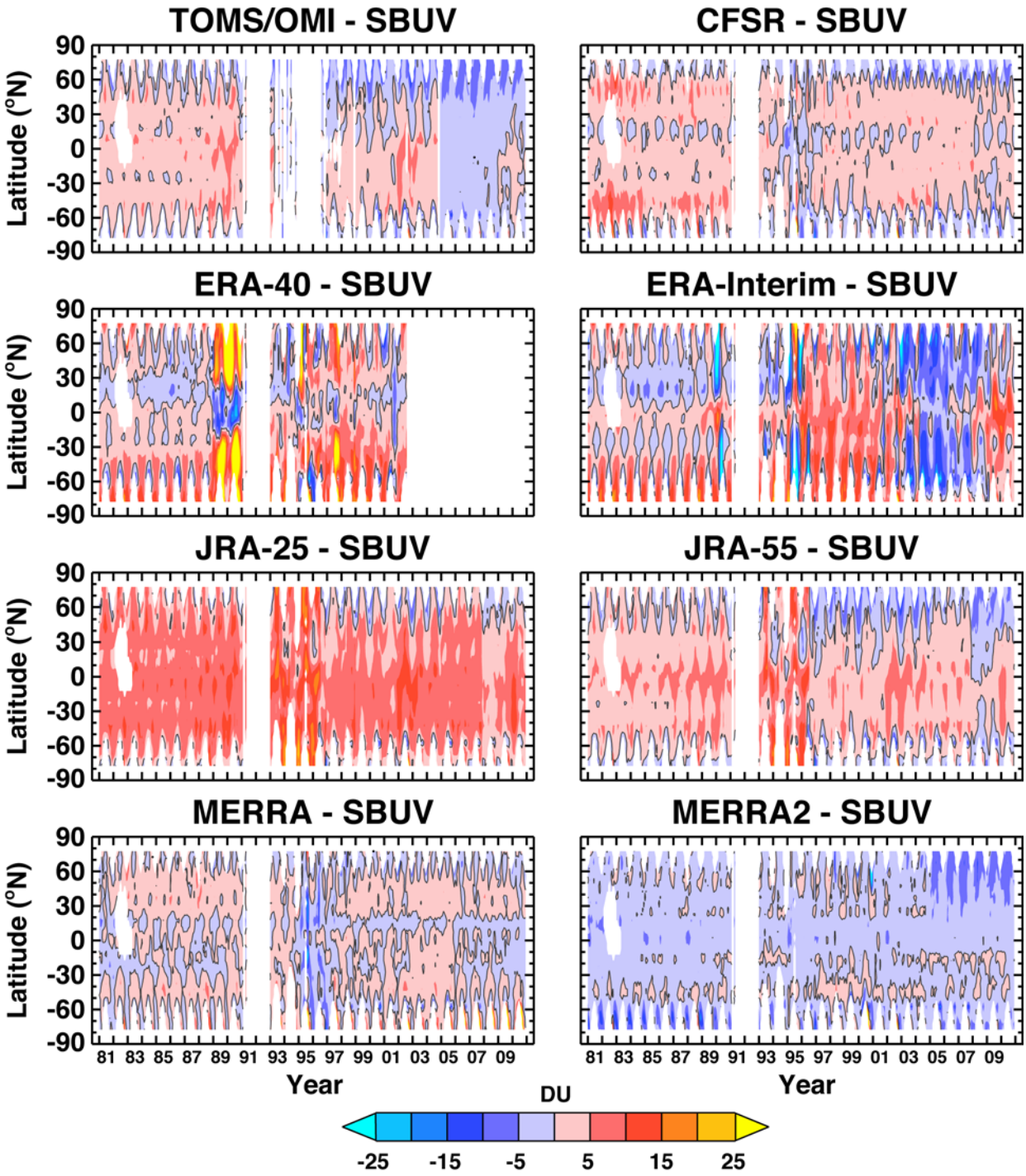

Figure 4.23. Zonal- and monthly-mean total column ozone differences of TOMS/OMI and reanalyses with SBUV.

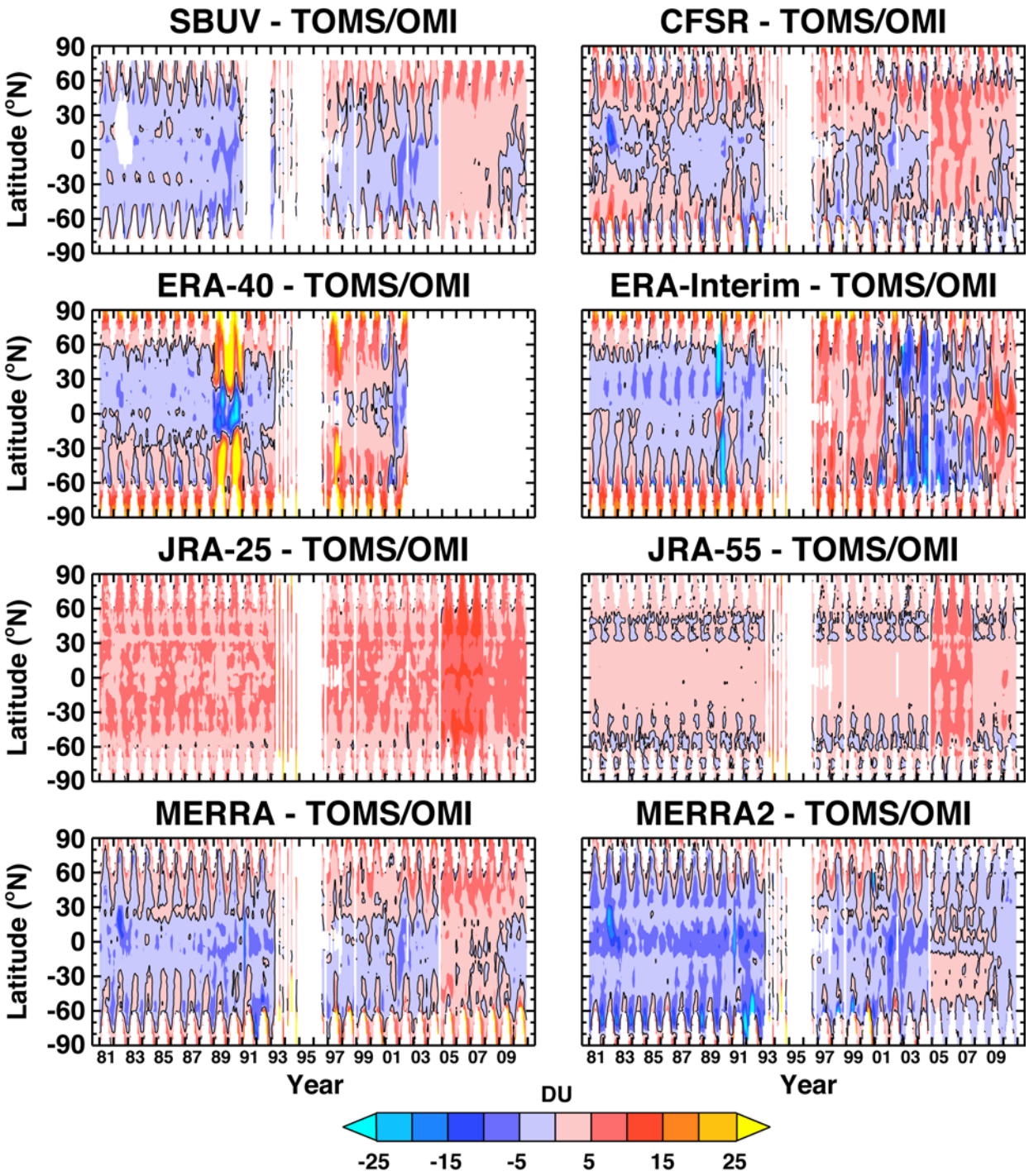

Figure 4.24. Zonal- and monthly-mean total column ozone differences of reanalyses with TOMS/OMI.

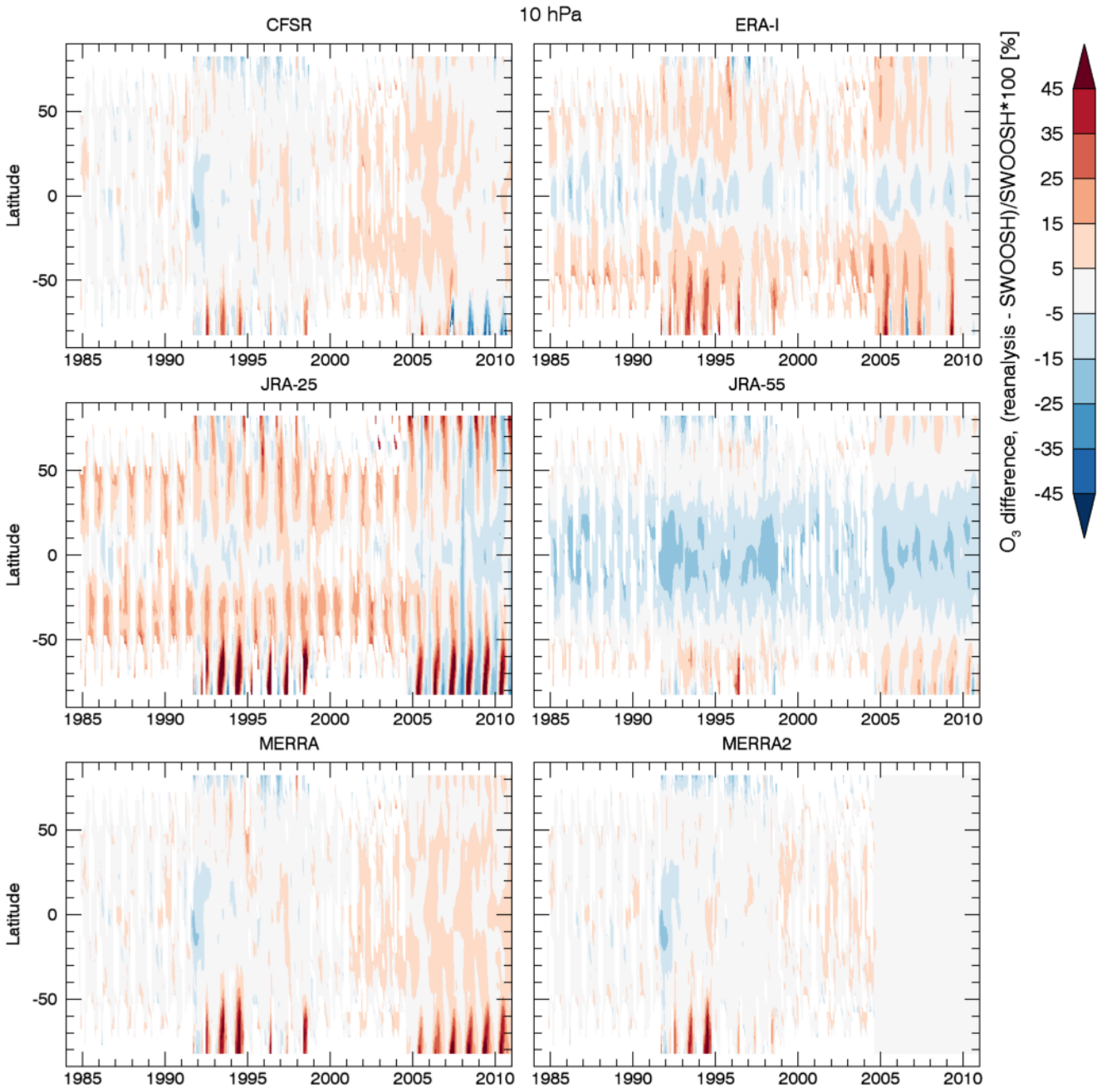

Figure 4.25. Plot of the percent differences between the reanalyses and the SWOOSH ozone record at 10 hPa.

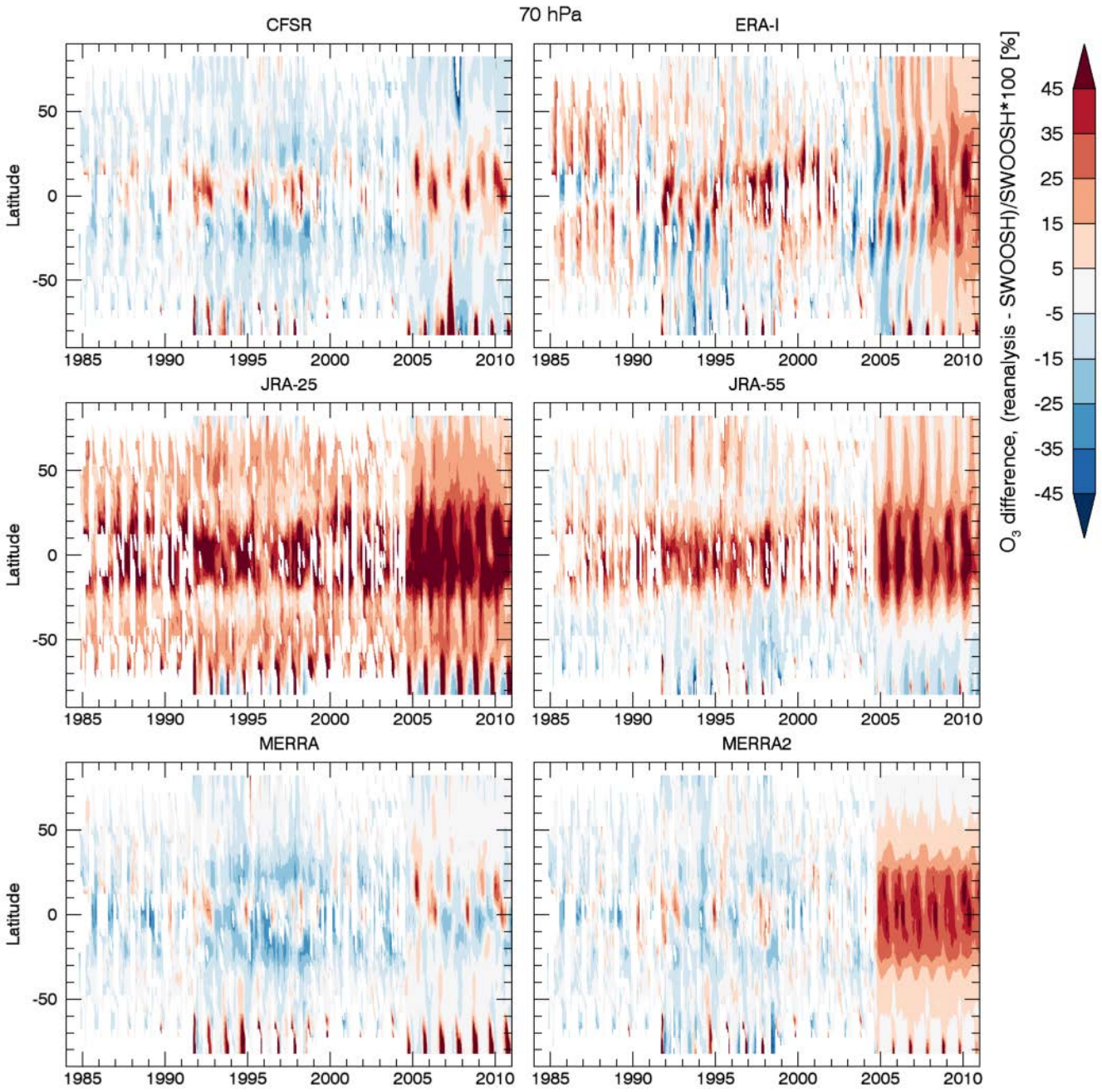

Figure 4.26. Same as Figure 4.25, but for 70 hPa.